DIFFERENTIATION BETWEEN ELECTRIC BREAKDOWNS AND DIELECTRIC BREAKDOWN IN THIN SILICON OXIDES

J. C. Jackson, T. Robinson, O. Oralkan, D. J. Dumin
Clemson University
Clemson, South Carolina 29634-0915

G. A. Brown
Texas Instruments, Inc.
Dallas, Texas 75265

ABSTRACT

It has been known for some time that non-destructive electric breakdowns precede destructive thermal dielectric breakdown. We have been studying both processes in oxides between 5 nm and 80 nm in thickness. We have shown that the electric breakdowns can trigger dielectric breakdown under certain conditions. This triggering of dielectric breakdown causes TDDB distributions to be non-unique. The TDDB distributions could be shifted to shorter times if a) the impedance of the test equipment was lowered and/or b) the capacitance of the test equipment was raised. The implications of this work will be discussed in terms of electric/dielectric breakdown models and practical circuit and device operation.

INTRODUCTION

It has been known for some time that non-destructive electric breakdowns precede destructive, thermal, dielectric breakdown in silicon oxides [1] [2] [3] [4] [5]. The electric/dielectric breakdown process has been described as a multi-step event, which has been summarized [2] [4] as follows. During the application of high voltages, traps are generated inside the oxide. These traps result in local high-current-density regions. These local high current regions lead to local oxide heating, thermal runaway, and electric breakdown. If the balance between the energy stored in the capacitor and the time decay of the current through the external electrical circuit is matched, the breakdown region can be open-circuited. This process repeats itself many times, at different locations, until a sufficiently low resistance path has been formed between cathode and anode to produce a shorting, thermal, breakdown. This final thermal breakdown is generally referred to as dielectric breakdown. Electric breakdowns have been measured to occur in about 1/10 of the time and at voltages as low as 1/2 of those required to produce thermal dielectric breakdowns [6]. These pre-breakdowns, soft-breakdowns, early-breakdowns, or quasi-breakdowns have received much study in the past several years [7] [8] [9] [10] [11]. It has been found that early breakdowns can be characterized by the noise associated with the electric breakdown events [12] [13] [14] [15].

Generally, when breakdown tests are performed, the time-to-breakdown results reported are the final, thermal, dielectric breakdown, not the earlier electric breakdowns, and are presented as time-dependent-dielectric-breakdown (TDDB) distributions. When measuring the breakdown voltage using ramp voltage tests, the applied voltage causing the breakdown is usually reported as the voltage required to produce dielectric breakdown, not the voltage at which the first electric breakdown occurs. Early breakdowns have not received much study, partially because, in the early days of integrated circuit technology, many of these breakdowns were defect related [16] [17]. However, the high quality of present integrated circuit technology has eliminated most of these defect dominated breakdowns and the electric breakdowns can now be considered to be intrinsic breakdowns and can be reliably studied in detail.

An engineering model of dielectric breakdown has been developed incorporating various TDDB distributions reported by different workers on different oxides using different test equipment [18]. Implicit in this model was the assumption that dielectric breakdown distributions measured in one facility could be reproduced in another facility, even though the measurement test stations might be different.

In this paper we will discuss electric and dielectric breakdowns. The two breakdowns will be described and correlated. It will be shown that the TDDB distributions measured on identical oxides at the same voltages were not unique, but depended on the details of the resistance and capacitance of the test station. The electric breakdown voltages

0-7803-3985-1/$10.00 © 1997 IEEE

measured during ramp voltage tests were significantly lower than the dielectric breakdown voltages. The impact of electric breakdowns on both dielectric breakdown theories and on practical device and circuit operations will be briefly discussed.

EXPERIMENTAL

Two different types of experiments measuring both electric and dielectric breakdowns were performed. In one set of experiments constant voltage TDDB distributions were measured while observing the surface of the oxides and recording both the steady current through the oxides and the transient voltages across the oxides. Different test equipments were used to apply the voltages and measure the currents during this experiment. In a second set of experiments the oxide voltages were ramped to breakdown and the surfaces of the wafers were observed and the transients that occurred prior to dielectric breakdown were recorded.

For the first set of experiments, high quality, 5 nm to 80 nm, oxides fabricated using commercial LOCOS processes on both n-type and p-type substrates were used. Constant-voltage TDDB distributions were measured using different measurement equipments. Both a relatively high impedance HP 4140b pAmeter and a low impedance, VIZ WP 711 voltage source were used. The voltages across the oxides were monitored using a Tektronix TDS520 oscilloscope during the TDDB measurements. Both the wave shapes and the times of the non-shorting electric breakdowns were recorded. On a separate set of oxides, the stress-induced-leakage-currents (SILCs) were measured after different numbers of non-shorting electric breakdowns had occurred. Photographs of the electric breakdown spots were taken on the thicker oxides.

For the second set of experiments, both the oxides described above and a set of 3 nm thick oxides fabricated on p-type substrates were used. The gate voltage was swept until dielectric breakdown occurred. A sensitive detector across the oxide detected current spikes associated with electric breakdowns prior to the occurrence of dielectric breakdowns. Some of the breakdown spots were photographed.

CONSTANT VOLTAGE BREAKDOWN RESULTS

The two types of breakdowns measured in this experiment have been described in Figure 1. Dielectric breakdown occurred when a precipitous, and permanent, increase in the oxide current was measured. The electric breakdowns shown in Figure 1 could be open circuited by the test equipment. The voltage across the oxide temporarily dropped when the electric breakdowns occurred as the capacitor discharged its energy. The gate voltage was then recharged from the voltage source when the electric breakdowns open-circuited [1] [2] [4]. These non-shorting electric breakdowns were usually accompanied by emission of light from the breakdown region, as have been observed by others [19] [20]. The transient voltage spikes became more frequent as dielectric breakdown was approached. Similar effects, including emission of light, have been reported for electric breakdowns in liquid dielectrics [21]. A typical voltage waveshape measured across a 40 nm thick oxide during one of the electric breakdown events has been shown in Figure 2. It should be noted that the electric breakdown spikes were not easily detectable using the HP 4140b pAmeter due to the slow response of the pAmeter. It was necessary to use the oscilloscope to detect the electric breakdowns.

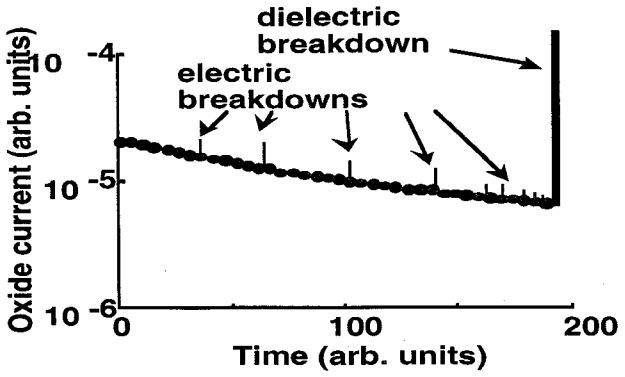

Figure 1 The current vs. time characteristics of an oxide being stressed at high voltage showing both the dielectric breakdown and the electric breakdowns.

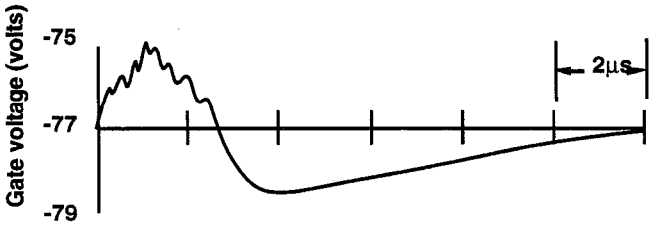

Figure 2 The voltage across 40 nm thick oxide during a typical electric breakdown event.

Photographs of the surface of the oxide described in Figure 2 have been shown in Figure 3 during the breakdown measurements. The last, and largest, spot measured on the wafer was the dielectric breakdown region. The spot patterns were usually different for the two polarities of stress voltage due to the different locations of asperities at the two electron injecting interfaces, particularly near the LOCOS edge [22].

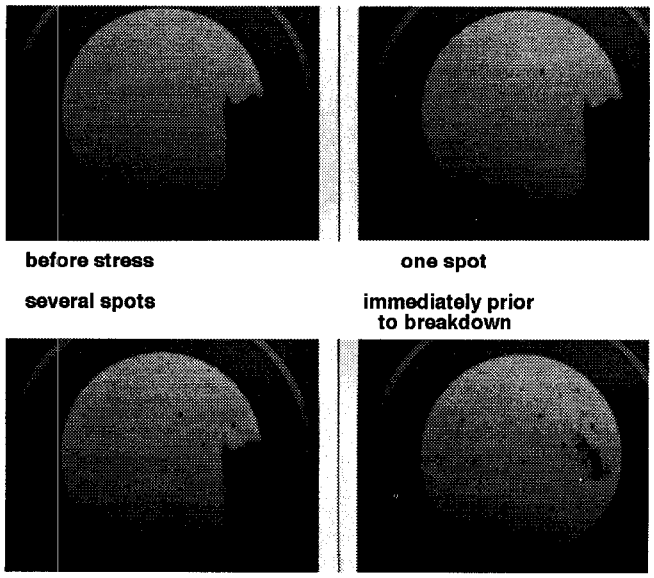

Figure 3 Breakdown spots photographed after electric breakdowns on 40 nm thick oxide.

In a separate experiment, the SILCs were measured during a breakdown measurement and have been shown in Figure 4, before any electric breakdowns had been observed, after the first electric breakdown, after about 10 electric breakdowns and just before dielectric breakdown occurred. These SILCs were comparable to those measured on thinner oxides during quasi-breakdown studies [11]. It has been shown that stress-induced leakage currents are proportional to the density of traps generated by the stresses [23], which seems to be consistent with the data shown in Figure 4.

Since it was clear that electric breakdowns were occurring prior to dielectric breakdown, it was decided to try to trigger some of the early electric breakdowns into dielectric breakdowns. The techniques that were used were to couple the 1/2 CV^2 energy stored in the oxide to the early breakdowns by a) lowering the impedance of the voltage source used to drive the current through the oxides and/or b) having more stored energy available for discharge by placing an external capacitor in parallel with the test structure and allowing this capacitor's energy to discharge through the electric breakdown region. A 0.1 μF tantalum capacitor was placed across the test oxide capacitor at the probes when more capacitive stored energy was desired. The total capacitor energy was not raised by increasing the test oxide area since it has been shown that intrinsic TDDB distributions are area dependent [24] due to the random nature of the statistics involved in the breakdown process [25]. Four TDDB distributions measured on 40 nm thick oxides on n-type substrates at +40.5 V have been shown in Figure 5. These TDDB distributions were measured using a) a HP 4140b pAmeter (40 KΩ) as the voltage source, b) a HP 4140b pAmeter with the 0.1 μF tantalum capacitor placed across the oxide, c) an VIZ WP 711 (4Ω) voltage source. The fourth time distribution shown in Figure 5 was the time of the first electric breakdown using the HP 4140b pAmeter as the voltage source and no capacitor across the oxide. The TDDB distributions measured on these identical oxides varied by about an order of magnitude and had similar slopes. A similar difference between non-destructive and destructive breakdowns has been reported [6]. Similar TDDB distributions were measured on other thicknesses of oxides.Three dielectric breakdown spots have been shown in Figure 6 for the three conditions described above.

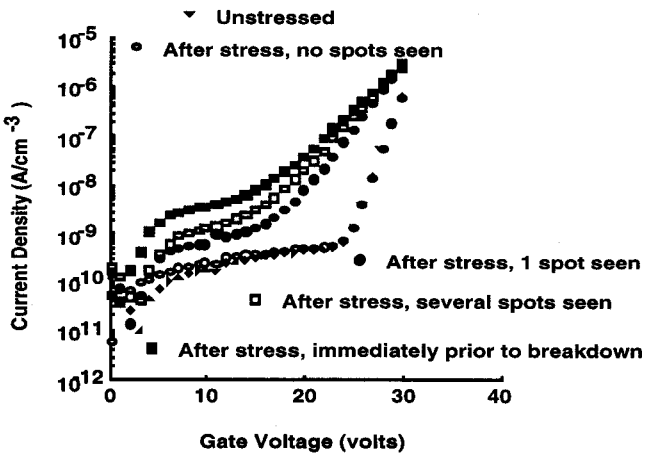

Figure 4 Low-level leakage currents measured on a 40 nm thick oxide.

RAMPED VOLTAGE RESULTS

Several of the oxides were sweep to breakdown at ramp rates of ±1 MV/sec. While transient voltage spikes were measured on all of the oxides, vis-

ible spots were recorded only on the thicker oxides. A detector circuit was set to indicate an electric breakdown whenever the logarithmic slope of the I-V characteristic increased by a factor of 3 over the average slope of the last 5 I-V recordings.

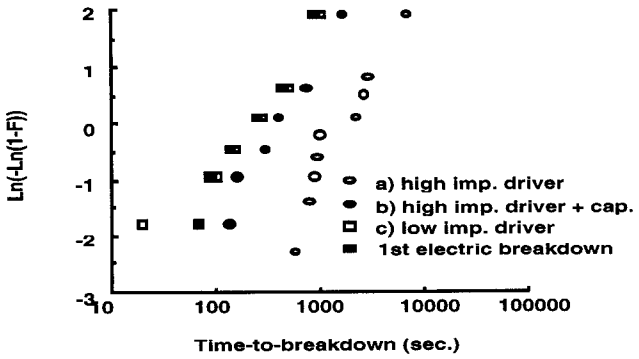

Figure 5 TDDB distributions measured on identical 40 nm thick oxides at 40.5 V using different test equipments.

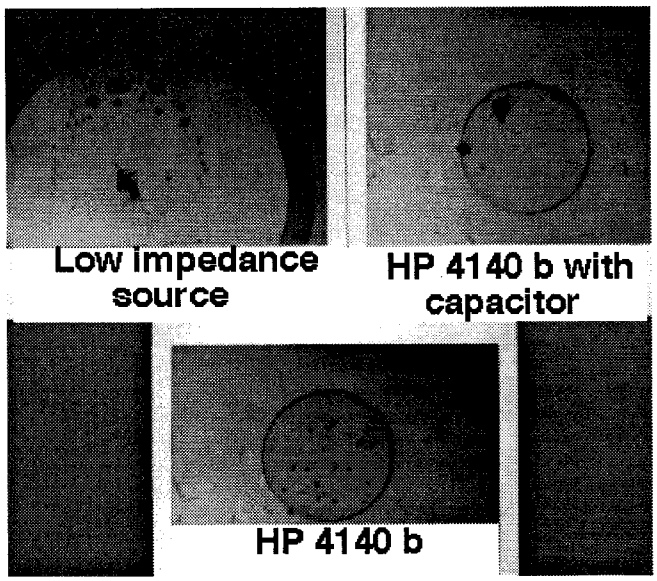

Figure 6 Breakdown spots photographed on 40 nm thick oxides when the HP 4140b pAmeter was used, with and without the external capacitor, and when the low impedance voltage source was used.

The I-V characteristics, to breakdown, of a 3 nm oxide has been shown in Figure 7, along with the change in the logarithmic slope. Dielectric breakdown occurred at 7.1 V and electric breakdown at 5.4 V. The breakdown voltage of this oxide would have been recorded as 5.4 V if the first electric breakdown were used as the breakdown criterion and would have been recorded as 7.1 V if dielectric breakdown had been used as the breakdown criterion. These data are similar to data that have been previously presented [6].

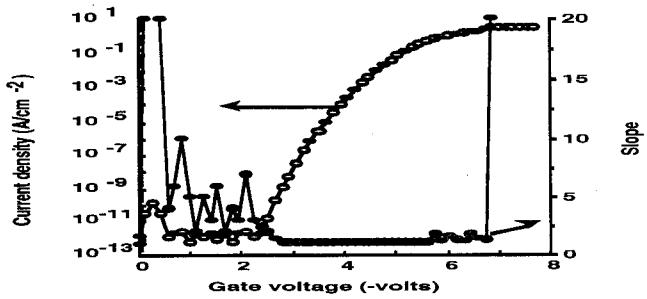

Figure 7 Ramped current-voltage characteristics of a 3 nm thick oxide along with the change in the logarithmic slope that occurred whenever an electric breakdown had occurred.

DISCUSSION OF RESULTS

The presence of both electric and dielectric breakdowns has been shown. These measurements support the work of others, who had shown that electric breakdowns occurred at shorter times and at lower voltages than did thermal, dielectric breakdown [6]. The triggering of some of these electric breakdowns into dielectric breakdown, by the use of an external capacitor or the use of a low impedance voltage source has shown that dielectric breakdown distributions, measured at the same voltages, are not unique. These results have several ramifications regarding the theoretical and practical aspects of dielectric breakdown measurements.

Much of the recent work on oxide breakdowns has concentrated on describing thermal dielectric breakdowns. A statistical model for dielectric breakdown has been proposed [25] and confirmed over a wide variety of oxide conditions [26]. This model and the confirmations were based on measuring the time, voltage, and thickness dependences of the trap generation inside the oxides prior to breakdown [27] and coupling the measured time dependences of the trap generation to the statistics of breakdown and the TDDB distributions [25]. In this model, breakdown was triggered when the local density of traps exceeded a critical value. It has been shown that parallel shifts in TDDB distributions to lower breakdown times, such as those shown in Figure 5, were predicted if the number of traps in the breakdown region remained constant and the breakdown area became larger [28]. A shorting breakdown would be ex-

pected to produce such a region. Thus, the statistical model of breakdown seems to account for the qualitative results reported above.

A recent model of dielectric breakdown, where the traps responsible for the triggering of breakdown must be aligned in space to produce a local high-current-density region, has been shown to be able to explain the thickness dependence of dielectric breakdown TDDB distributions [29]. Both of the theoretical models of dielectric breakdown [25] [29] appear to be sufficiently robust to predict electric and/or dielectric breakdowns. The only differences that need to be applied, when using these models is to differentiate between the two breakdowns, is to change the number of traps required to trigger a breakdown and to change the cross-sectional area of the breakdown region. The experimental confirmations of these theories will require that both electric and dielectric breakdowns are measured. Any, more complete, model of electric/dielectric breakdown, that is developed in the future, must include the thermal geometry of the oxide, including a transient analysis of the circuitry used to make the measurements. This more complete theory awaits development.

It has been observed by many workers that the dielectric breakdown field decreases as the oxide thickness increases [30]. This effect has often been attributed to the higher likelihood of including a defect in a thicker oxide and, thus, the triggering of an extrinsic breakdown. Based on the work reported here there may be an additional effect due to the energy stored in the capacitor causing the breakdown field to drop as the oxide thickness increases. The energy stored in the oxide, E_n, is given as

$$E_n = 1/2\ C\ V^2 = 1/2\ \varepsilon_s\ A\ E_{ox}\ V, \qquad (1)$$

where C is the oxide capacitance, V is the applied voltage, ε_s is the dielectric constant of the oxide, A is the capacitor area, and E_{ox} is the oxide field, approximated as the oxide voltage divided by the oxide thickness. At a constant oxide field and as the oxide thickness is increased, the energy stored in the capacitor increases. It was shown in Figure 5 that the time-to-breakdown decreased as the stored energy in the oxide increased. A similar effect may be lowering the breakdown field of the thicker oxides leading to lower breakdown fields for thicker oxides.

The current-voltage characteristics, to breakdown, of oxides of different thicknesses have been shown in Figure 8. The electric field at dielectric breakdown was smaller in the thicker oxides, in agreement with previous work of others [30]. However, the energy stored in the oxide, at the breakdown voltage, increased as the oxide thickness increased and may be part of the reason lower breakdown fields have been associated with dielectric breakdown in thicker oxides.

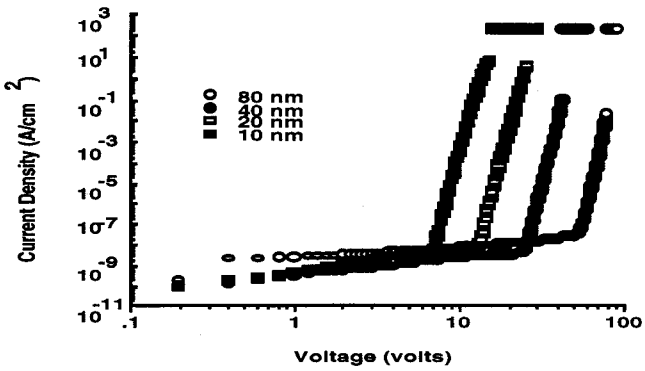

Figure 8 Ramped current-voltage characteristics of different thicknesses of oxides showing the dielectric breakdown.

The energy stored in the capacitor, at the breakdown voltage, has been plotted as a function of oxide thickness in Figure 9. In light of the differences observed here between electric and dielectric breakdowns, it is necessary to reconsider the thickness dependences of breakdown fields.

It is believed that these non-destructive electric breakdowns are possibly the cause of the over-erase upsets in EEPROMs when Fowler-Nordheim tunneling is used for erasing [31]. During the erase cycle electric breakdowns trigger upsets in a few of the cells, but do not, in general, permanently damage any individual cell. However, once a cell has had an electric breakdown, there may be a higher probability that a subsequent electric breakdown can occur near the first electric breakdown region and trigger another upset in this cell. The extra current associated with the electric breakdowns can over-erase the cell and cause the skew of the erased cells' threshold voltages.

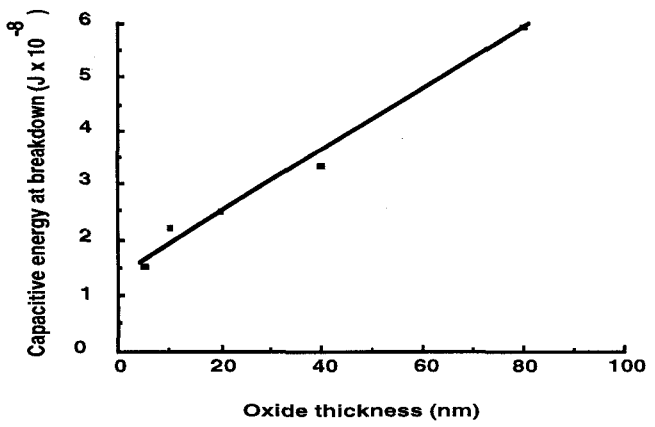

Figure 9 The stored energy in the oxides as a function of oxide thickness at the breakdown voltages shown in Figure 8.

CONCLUSIONS

It has been shown that both electric and dielectric breakdowns can be observed in oxides using both constant voltage and ramped voltage measurements. These electric breakdowns can be triggered into dielectric breakdown if appropriate modifications are made to the external measurement circuitry. Thus, TDDB distributions at a constant voltage are not unique. The two statistical models of breakdown appear to be sufficiently robust to describe both electric and dielectric breakdowns. These electric breakdowns may be the cause of upsets in EEPROMs when F-N tunneling is used to erase the cells.

ACKNOWLEDGEMENTS

Mr. Jackson, Mr. Robinson, and Mr. Oralkan were, in part, supported by Texas Instruments Undergraduate and Graduate Fellowships. Mr. Robinson's present address is EECS Dept., University of California, Berkeley, CA.

REFERENCES

1. N. Klein, IEEE Trans. on Electron Devices **ED-13**, 788, 1966.
2. N. Klein, "Switching and Breakdown in Films", Thin Solid Films **7**, 149, 1971.
3. M. Shatzkes, et al. Appl. Phys. **45**, 2065, 1974.
4. P. Solomon, J. Vac. Sci. Technol. **14**, 1122, 1977.
5. D. R. Wolters and J. J. Van Der Schoot, Philips J. Res. **40**, 164, 1985
6. M. Shatzkes and M. Av-Ron, IEEE/IRPS Tutorial #6, 1992 and references listed therein.
7. B. Neri, et al, Appl. Phys. Lett. **51**, 2167, 1987.
8. K. R. Farmer, et al, Appl. Phys. Lett. **52**, 1749, 1988.
9. H. Satake, et al, Appl. Phys. Lett. **69**, 1128, 1996.
10. M. Depas, et al, IEEE Trans. on Electron Devices **ED-43**, 1499, 1996.
11. T. Yoshida, et al, Inter. Conf. on Solid State Dev. and Mat., 1996.
12. R. Saletti, et al, IEEE Trans. on Electron Devices **ED-37**, 2411, 1990.
13. R. Saletti and B. Neri, IEEE Trans. on Instrumentation and Measurement **IM-41**, 123, 1992.
14. B. Neri, et al, Microelectron. Reliab. **35**, 529, 1995.
15. G. B. Alers, et al, "Tunneling current noise in thin gate oxides", Appl. Phys. Lett. **69**, 2885, 1996.
16. J. R. Monkowski, Microcontamination, 37, February-March, 1984.
17. D. R. Wolters and J. J. Van Der Schoot, Philips J. Res. **40**, 115, 1985.
18. I. C. Chen and C. Hu, IEEE Electron Device Letters **EDL-8**, 140, 1987.
19. Y. Uraoka and K. Tsuji, IEICE Trans. Electron **E76-C**, 519, 1993.
20. M. Mankos, et al, Phys. Rev. Lett. **76**, 3200, 1995.
21. P. Barmann, et al, J. Phys. D: Appl. Phys. **29**, 1188, 1996.
22. Y. Hokari, IEEE Trans. on Electron Devices **ED-35**, 1299, (1988).
23. D. J. Dumin and J. R. Maddux, IEEE Trans. on Electron Devices **ED-40**, 986, 1993.
24. R.-P. Vollertsen and W. G. Kleppmann, Proc IEEE/ICMTS 1991, 75.
25. J. Sune, et al, Thin Solid Films **185**, 347, 1990.
26. D. J. Dumin, et al, IEEE Trans. on Electron Devices **ED-41**, 1570, 1994.
27. R. S. Scott, et al, IEEE Trans. on Electron Devices **ED-43**, 1133, 1996.
28. R. Subramoniam, et al, Tech. Digest 1992 IEDM, 135.
29. R. Degraeve, et al, Proc. of the 1995 Int. Rel. Physics Symp. **34**, 44, 1996.
30. E. Harari, Appl. Phys. Lett. **30**, 601, 1977.
31. C. Dunn, et al, Proc. of the 1995 Int. Rel. Physics Symp. **33**, 299, 1994.